Dynamic biological adhesion: mechanisms for controlling attachment during locomotion

Supplementary information

Walter Federle[1] and David Labonte[2]

[1]Department of Zoology, University of Cambridge, United Kingdom
[2]Department of Bioengineering, Imperial College, United Kingdom

Statistics

[1, 1]

Table S 1: Detailed results for the regression lines showing in Fig. 2 (a-c), (e-g) in the main manuscript. All regression coefficients are the result of major axis regressions. The values in brackets indicate the 95% confidence intervals of the regression coefficients. The data for dock beetles are from single-pad measurements (D Labonte & JMR Bullock 2015, unpublished data)

	Species	System	Intercept in mN	Slope (SMA)	Source
Vertebrates	*Gecko gecko*	Hairy & Dry	5.12 (-2.54; 12.81)	0.41 (0.40; 0.43)	[2]
	Litoria caerulea	Smooth & Wet	0.95 (-4.41; 6.31)	0.44 (0.38; 0.52)	[3]
Invertebrates	*Gastrophysa viridula*	Hairy & Wet	0.06 (-0.02; 0.14)	0.63 (0.51; 0.79)	–
	Carausius morosus	Smooth & Wet	0.46 (0.36, 0.56)	0.50 (0.48, 0.52)	[4]
	Nauphoeta cinerea	Smooth & Wet	0.43 (0.22; 0.63)	0.51 (0.47; 0.55)	[5]
	Oecophylla smaragdina	Smooth & Wet	0.19 (0.05; 0.32)	0.63 (0.60; 0.66)	[6]

Image sources for Figure 1

Image sources (left to right): Blue mussel (*Mytilus edulis*) with byssus threads, [7]; Adult barnacle (*Balanus amphitrite*) attached to glass (courtesy of Nicholas Aldred); Sea star (*Asterias rubens*) tube feet (courtesy of Elise Hennebert); Flatworm (*Macrostomum lignano* [8]; Barnacle cyprid (*Semibalanus balanoides* [9]; Net-winged midge larva (*Hapalothrix lugubris*; courtesy of Victor Kang); Leech (*Hirudo medicinalis*; courtesy of Plant Biomechanics Group Freiburg); Goby fish (*Sicyopterus stimpsoni*; courtesy of Takashi Maie); Tokay Gecko (*Gekko gecko*, courtesy of Kellar Autumn); Tree frog (*Litoria caerulea*; courtesy of Thomas Endlein); *Camponotus schmitzi* ant [10], photo by Thomas Endlein; Erythracarid mite (*Paratarsotomus macropalpis*, courtesy of Jonathan Wright). These mites can run with stride frequencies of up to 111 Hz at 45°C [11, 12]; they can also effectively climb up smooth glass surfaces (Jonathan Wright, pers. comm.).

Tape peeling models

We consider peeling a thin strip of adhesive tape with width w, thickness h, Young's modulus E and strain energy release rate G, by applying a force F at an angle ϕ relative to the horizontal. We assume that the length of the tape is infinite, that its bending stiffness is negligible, and

that peeling is in steady-state. The critical force required to peel the tape can be found from a virtual work argument, as shown by numerous authors in the past [13–15]. Here, we only briefly state the main results, and refer the reader to the supplementary material presented in [16] for a detailed derivation of various peel models. Balancing the elastic, potential and adhesive work done during peeling yields [14]:

$$P^2 + 2P\left(1-\cos\phi\right) - 2\frac{G}{Eh} = 0 \tag{1}$$

where we introduced $P = \frac{F}{Ehw}$. The roots are:

$$P_{1,2} = \cos\phi - 1 \pm \sqrt{\left[1-\cos\phi\right]^2 + 2\frac{G}{Eh}} \tag{2}$$

Only the upper root is positive, and the maximum peel force occurs at $\phi = 0°$, for which $F/w = \sqrt{GEh}$. As biological adhesive pads are thin and soft, tape stretching severely limits the maximum force compared to thicker and stiffer industrial tapes. The limiting effects of tape stretching can however be circumvented if the tapes are 'pre-stretched' while still in contact with the surface. In the presence of such a 'pre-strain', $\varepsilon_0 = \frac{F_0}{Ehw}$, a virtual work argument yields [16]:[1]

$$P^2 + 2P\left[1-(1-\varepsilon_0)\cos\phi\right] + \varepsilon_0^2 - 2\frac{G}{Eh}(1+\varepsilon_0) = 0 \tag{3}$$

The roots are:

$$P_{1,2} = (1+\varepsilon_0)\cos\phi - 1 \pm \sqrt{\left[1-(1+\varepsilon_0)\cos\phi\right]^2 - \varepsilon_0^2 + 2\frac{G}{Eh}(1+\varepsilon_0)} \tag{4}$$

Three key differences between expressions 2 and 4 are noteworthy. First, the peel force is maximal if the pre-strain takes a value:[2]

$$\varepsilon_{\max} = \frac{1}{\zeta\left(1-\cos\phi\right)} \tag{5}$$

where we introduced $\zeta = Eh/G$, a dimensionless parameter which may be interpreted as the ratio of elastic to adhesive work during peeling [16]. With this pre-strain, the critical peel force is:

$$P = \frac{1}{\zeta\left(1-\cos\phi\right)} \tag{6}$$

which is equivalent to the result for a rigid tape, $F/w = G\left(1-\cos\phi\right)^{-1}$ [13]. This result may also be understood intuitively: the maximum force enhancement occurs if the tape does *not stretch at all* upon detachment, making a deformable tape behave as if it was rigid; the required pre-strain is the strain caused by the force required to peel a rigid tape, an argument which also yields the above result. Under the plausible assumption that the pads are stretched by the shear component of the applied force, the arising strain will be close to this 'ideal' strain, $\varepsilon_0 \approx \varepsilon_{\max} = \frac{1}{\zeta(1-\cos\phi)}$ [16]. An attachment system utilising pre-stretching in this way would then

[1] Note that this expressions differs from previous solutions by an additional term $2\frac{G\varepsilon_0}{Eh}$. This term arises because stretching increases the total length of the tape, and hence its interfacial area with the substrate. The difference is negligible if $\zeta = Eh/G$ is large, which is the case for most man-made tapes, but not for biological adhesive pads [for a more detailed discussion, see ref. 16].

[2] This result is found by setting the derivative with respect to ε_0 equal to zero.

be 'self-maximising' by design. Note that the peel force diverges as the peeling angle approaches 0°; this is of course unphysical, and 'real' tapes will deform non-elastically, fracture and/or slide instead [15, 16].

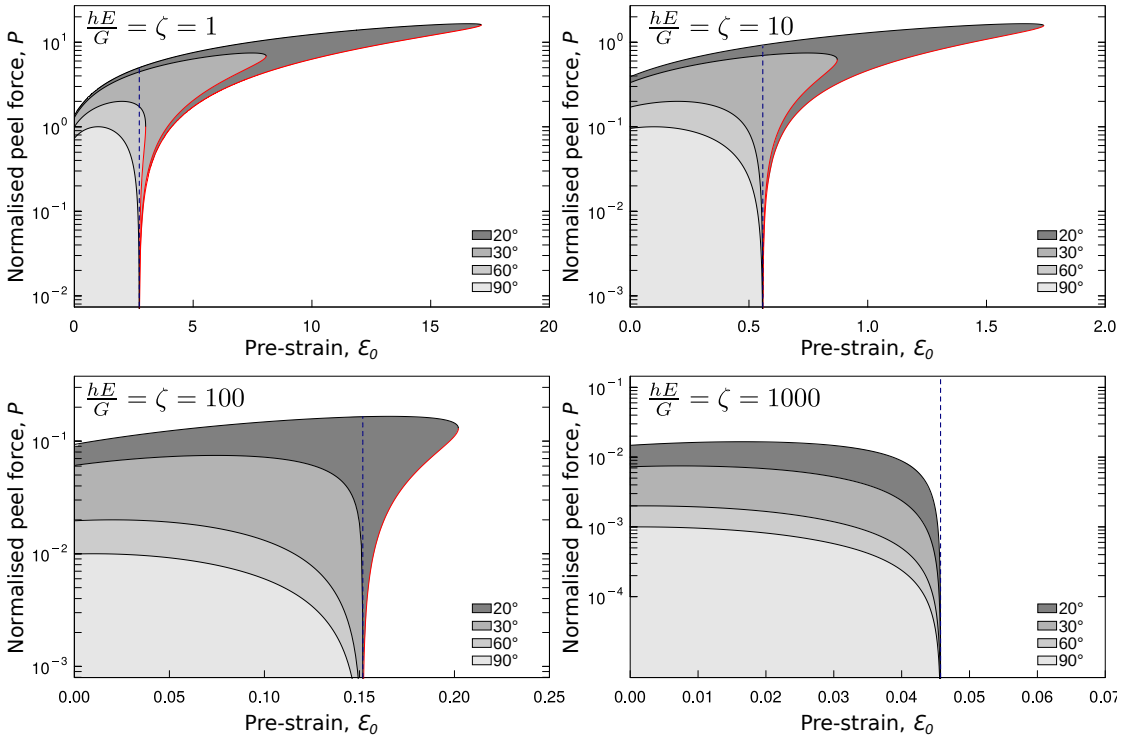

Figure S 1: Stability envelopes for the peeling of a thin tape as a function of tape 'pre-strain' ε_0. The coloured areas correspond to stable attachment, the black lines show the upper root of eq. 3, i. e. the critical peel force, while the red lines show the lower root of eq. 3, i. e. the minimum force required to stabilise the tape against being peeled off the surface. Note that this lower root is only positive if the pre-strain exceeds a critical value, $\varepsilon_0 > \frac{1}{\zeta}\left(1+\sqrt{1+2\zeta}\right) = \varepsilon_{\min}$, which is indicated in the plots by the blue dashed line. A tape stretched to this pre-strain would spontaneously detach in the absence of an external force, as the strain energy stored in the tape is equal to the gain in adhesive energy associated with the creation of new surface area. Once this pre-strain is exceeded, the strain energy is sufficient to detach the pads without applying an external force; the applied force simply has to drop below the value given by the lower root of eq. 3. Note that this condition is increasingly hard to meet for large values of ζ.

Second, while classic tape peeling always requires the application of an external force, a pre-stretched tape can detach spontaneously, i. e. in the absence of external forces. In order to see why, consider peeling the tape at an angle $\phi = 0$. The lower root is zero if:[3]

$$\varepsilon_{\min} = \frac{1}{\zeta}\left(1+\sqrt{1+2\zeta}\right) \tag{7}$$

Qualitatively, this result may be understood by thinking of the tape as a linear spring stretched

[3]For large ζ, this expression simplifies to $\sqrt{2\zeta^{-1}}$, which is the result given by Chen et al. [17]. It can also be found by setting the square root in eq. 4 equal to zero.

before attaching it to a surface. If the strain energy stored in the spring exceeds the reduction in energy associated with contact formation, the spring will detach, minimising the total energy in the system. The spring can however be stabilised if a sufficiently large force is applied to the detached parts, so that not all strain energy is released upon detachment. This physical insight is reflected in third, the fact that expression 3 can have two positive roots, as first discussed by Chen et al. [17]. The upper root corresponds to the critical force required to peel the tape; the lower root is the minimum force required to stabilise the tape against peeling as a result of the residual strain energy stored in it. If both roots are positive, adhesion will only be stable if $P_1 > P > P_2$. The somewhat complex relationship between the involved variables can be visualised by plotting 'stability envelopes', which highlight combinations of P and ε_0 which correspond to stable attachment (see Fig S 1). The lower root will be positive if and only if $\varepsilon_0 > \varepsilon_{\min}$.

Such (large) pre-tension may arise in pads by a variety of mechanisms, but most likely as a consequence of the large shear forces experienced during low-angle peeling [16–18]. These forces can be sufficiently large to cause whole pads to slide, and such sliding events must be preceded by partial sliding of the pads close to the peel front, where the shear stress is largest [16, 18]. Pads may also be stretched due to rapid sliding events during pad detachment, which can be accompanied by 'crack healing', i. e. the re-attachment of detached and stretched parts of the pads [16]. In both cases, pre-tension is not in active control of the animal, but arises as a direct consequence of pad engagement. Even if these mechanisms were sufficient to achieve such high levels of pre-strain, stretching by sliding would imply that they are present only on the proximal side of the contact zone but not on the distal side where strain levels decay to zero [18]. Moreover, the pre-strain model assumes that unloading before detachment is sufficiently fast, so that the pre-stretch does not revert by sliding (and hence dissipate the stored elastic energy).

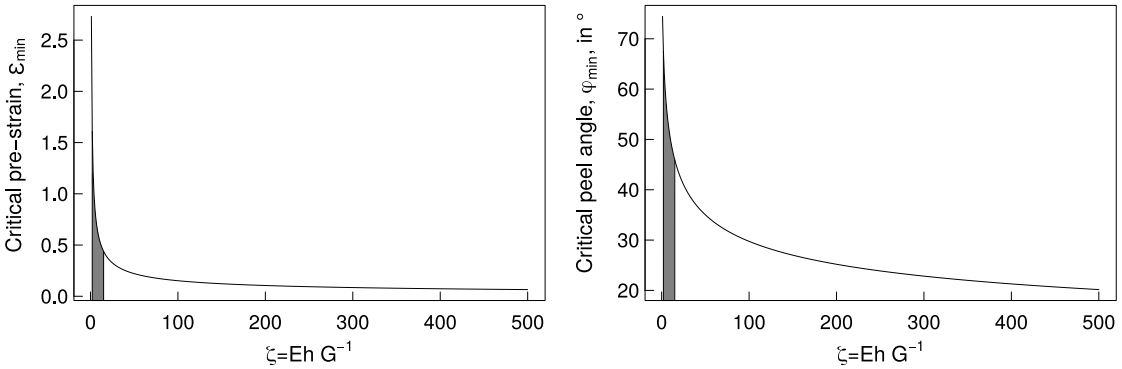

Figure S 2: (a) In order to use residual strain energy to drive spontanous detachment, the pre-strain in a thin strip of tape must exceed a critical value $\varepsilon_{\min}$. For soft and thin tapes, this value is large, suggesting a lower limit for ζ for which strain energy can be realistically exploited. (b) This critical minimum strain can only be reached if the tape is peeled at an angle smaller than $\phi_{\max}$. It may be desirable to increase the range of angles for which strain energy can be used to drive detachment, which would then also suggest an upper bound on ζ. The grey area in both plots highlights the approximate range for ζ in biological adhesive pads [16].

Notwithstanding the speculative nature of the argument, it is instructive to briefly consider the 'design criteria' for a tape or pad which may benefit from the effects of pre-tension. For small values of ζ, $\varepsilon_{\min}$ becomes exceedingly and perhaps unrealistically large (see Fig. S 2(a)). For large values of ζ in turn, the force required to reach $\varepsilon_{\min}$ diverges, and, perhaps more crucially, the release mechanism can only be triggered if pads are sheared at smaller and smaller angles,

limiting the kinematics of the detachment process [see Fig. S 1 & S 2(b)), and ref. 17]. The maximum peel angle which can satisfy $\varepsilon_0 > \varepsilon_{\min}$ is

$$\phi_{\max} = \cos^{-1}\left(\frac{1}{1+\varepsilon_{\min}}\right) \tag{8}$$

which can be found by setting the square root in eq. 4 equal to zero. In other words, this is the angle at which the two roots of eq. 4 merge into one solution. Utilising pre-tension for both enhancing attachment and driving detachment may only be possible for a limited range of values for ζ. Further research is required to establish if animal adhesive pads fall within this range.

Table S 2: Overview of different temporary adhesive systems of animals, comparing adhesive mechanism, contact size, locomotion speed and (defined here as the inverse of the time of one complete pad attachment-detachment cycle). All values are approximate.

	Taxon	Environment	Adhesive mechanism	Pad Type	Contact size	Speed ($mm\,s^{-1}$)	Stride frequency (s^{-1})	Sources
Glue-based	Flatworm (*Macrostomum lignano*)	water	glue-like adhesive, and release agent	Adhesive cell organs	26 μm^2	–	0.14	[19]
	Sea star (*Asterina rubens*)	water	glue-like adhesive, and release agent	tube feet	1.3 mm^2	1	0.02-0.1	[20, 21]
	Barnacle cyprids (*Semibalanus balanoides*)	water	viscous adhesive secretion & interfacial forces	antennulary attachment discs, covered in villi	480 μm^2 (adhesive disc), <0.1 μm^2 (villi)	0.1	0.12-0.4	[9, 22–25]
Suction	Net-winged midge larva (*Liponeura cinerascens*)	water	suction	smooth	0.04-0.15 mm^2	0.2-0.8	0.4-1.6	[26, 27]
	Goby fish (*Sicyopterus stimpsoni*)	water	suction	oral and pelvic suction pads	4.5-5.5 mm^2	6	4.4 (inching)	[28]
	Leech (*Hirudo medicinalis*)	air & water	suction	suction pad	19-24 mm^2	13	0.10-0.15	[29, 30]
Interfacial forces	Gecko (*Hemidactylus garnotii*)	air	Interfacial forces (dry)	fibrillar	0.02 μm^2 (spatula) | 19 mm^2 (toe)	290-790	12.5	[31, 32]
	Spider (*Cupiennius salei*)	air	Interfacial forces (wet)	fibrillar	0.2 μm^2 (spatula) | 1 mm^2 (claw tuft)	600	8	[33, 34]
	Tree frog (*Litoria caerulea*)	air	Interfacial forces (wet)	smooth	5.3 mm^2	13-166 (vertical)	0.7-1.5	[35, 36]
	Fly (*Calliphora vicina*)	air	Interfacial forces (wet)	fibrillar	0.5-2 μm^2 (seta) | 10000-40000 μm^2 (pad)	–	13.9	[37, 38]
	Ant (*Camponotus schmitzi*)	air	Interfacial forces (wet)	smooth	4500 μm^2	61.7	13.6 (maxima up to 30)	[39, 40]
	Ant (*Camponotus floridanus*)	air	Interfacial forces (wet)	smooth	4500 μm^2	10-50 (inverted)	4-5	[6]
	Ant (*Oecophylla smaragdina*)	air	Interfacial forces (wet)	smooth	27000 μm^2	10-40 (inverted)	3-4	[6]

References

1. Giribet, G. and Edgecombe, G.D. (2019). The Phylogeny and Evolutionary History of Arthropods. Current Biology *29*, R592–R602.

2. Autumn, K., Dittmore, A., Santos, D., Spenko, M., and Cutkosky, M. (2006). Frictional adhesion: a new angle on gecko attachment. J Exp Biol *209*, 3569–3579.

3. Endlein, T., Ji, A., Samuel, D., Yao, N., Wang, Z., Barnes, W.J.P., Federle, W., Kappl, M., and Dai, Z. (2013). Sticking like sticky tape: tree frogs use friction forces to enhance attachment on overhanging surfaces. J R Soc Interface *10*, 20120838.

4. Labonte, D., Clemente, C.J., Dittrich, A., Kuo, C.Y., Crosby, A.J., Irschick, D.J., and Federle, W. (2016). Extreme positive allometry of animal adhesive pads and the size limits of adhesion-based climbing. PNAS *113*, 1297–1302.

5. Dirks, J.H. (2009). Mechanisms of fluid-based adhesion in insects. Ph.D. thesis, University of Cambridge.

6. Endlein, T. (2007). Haftung und Fortbewegung: Kontrollmechanismen von Adhäsionskräften bei Ameisen. Ph.D. thesis, Julius-Maximilians-Universität Würzburg.

7. Waite, J.H. (1991). Mussel beards: a coming of age. Chemistry & Industry 2 , 607–611.

8. Verdoodt, F., Willems, M., Mouton, S., De Mulder, K., Bert, W., Houthoofd, W., Smith, Julian, I.I.I., and Ladurner, P. (2012). Stem cells propagate their DNA by random segregation in the flatworm *Macrostomum lignano*. PLOS ONE *7*, e30227.

9. Phang, I.Y., Aldred, N., Clare, A.S., and Vancso, G.J. (2007). Towards a nanomechanical basis for temporary adhesion in barnacle cyprids (*Semibalanus balanoides*). J R Soc Int *5*, 397–402.

10. Thornham, D.G., Smith, J.M., Ulmar Grafe, T., and Federle, W. (2012). Setting the trap: cleaning behaviour of *Camponotus schmitzi* ants increases long-term capture efficiency of their pitcher plant host, *Nepenthes bicalcarata*. Funct Ecol *26*, 11–19.

11. Wu, G.C., Wright, J.C., Whitaker, D.L., and Ahn, A.N. (2010). Kinematic evidence for superfast locomotory muscle in two species of teneriffiid mites. J Exp Biol *213*, 2551.

12. Rubin, S., Young, M.H.Y., Wright, J.C., Whitaker, D.L., and Ahn, A.N. (2016). Exceptional running and turning performance in a mite. J Exp Bio *219*, 676–685.

13. Rivlin, R. (1944). The effective work of adhesion. Paint Technol *9*, 215–216.

14. Kendall, K. (1975). Thin-film peeling – the elastic term. J Phys D: Appl Phys *8*, 1449–1452.

15. Begley, M.R., Collino, R., Israelachvili, J.N., and McMeeking, R.M. (2013). Peeling of a tape with large deformations and frictional sliding. J Mech Phys Solids *61*, 1265–79.

16. Labonte, D. and Federle, W. (2016). Biomechanics of shear-sensitive adhesion in climbing animals: peeling, pre-tension and sliding-induced changes in interface strength. J R Soc Interface *13*, 20160373.

17. Chen, B., Wu, P., and Gao, H. (2009). Pre-tension generates strongly reversible adhesion of a spatula pad on substrate. J R Soc Interface *6*, 529–537.

18. Cheng, Q.H., Chen, B., Gao, H.J., and Zhang, Y.W. (2011). Sliding-induced non-uniform pre-tension governs robust and reversible adhesion: a revisit of adhesion mechanisms of geckos. J R Soc Interface *9*, 283–91.

19. Lengerer, B., Pjeta, R., Wunderer, J., Rodrigues, M., Arbore, R., Schärer, L., Berezikov, E., Hess, M.W., Pfaller, K., and Egger, B. (2014). Biological adhesion of the flatworm *Macrostomum lignano* relies on a duo-gland system and is mediated by a cell type-specific intermediate filament protein. Frontiers Zool *11*, 12.

20. Kerkut, G. (1953). The forces exerted by the tube feet of the starfish during locomotion. J Exp Biol *30*, 575–583.

21. Santos, R., Gorb, S., Jamar, V., and Flammang, P. (2005). Adhesion of echinoderm tube feet to rough surfaces. J Exp Biol *208*, 2555–2567.

22. Crisp, D. (1976). Settlement responses in marine organisms. In Adaptation to environment. Essays on the physiology of marine animals, R. Newell, ed. (Butterworths, London), pp. 83–124.

23. Lagersson, N. and Høeg, J. (2002). Settlement behavior and antennulary biomechanics in cypris larvae of *Balanus amphitrite* (Crustacea: Thecostraca: Cirripedia). Mar Biol *141*, 513–526.

24. Aldred, N., Høeg, J.T., Maruzzo, D., and Clare, A.S. (2013). Analysis of the behaviours mediating barnacle cyprid reversible adhesion. PLoS One *8*, e68085.

25. Aldred, N., Alsaab, A., and Clare, A.S. (2018). Quantitative analysis of the complete larval settlement process confirms Crisp's model of surface selectivity by barnacles. Proc R Soc B *285*, 20171957.

26. Frutiger, A. (1998). Walking on suckers: New insights into the locomotory behavior of larval net-winged midges (Diptera: Blephariceridae). J N Am Benthol Soc *17*, 104–120.

27. Frutiger, A. (2002). The function of the suckers of larval net-winged midges (Diptera: Blephariceridae). Freshwater Biol *47*, 293–302.

28. Schoenfuss, H.L. and Blob, R.W. (2003). Kinematics of waterfall climbing in Hawaiian freshwater fishes (Gobiidae): vertical propulsion at the aquatic-terrestrial interface. J Zool *261*, 191–205.

29. Stern-Tomlinson, W., Nusbaum, M., Perez, L., and Kristan, W. (1986). A kinematic study of crawling behavior in the leech, *Hirudo medicinalis*. J Comp Physiol A *158*, 593–603.

30. Kampowski, T., Eberhard, L., Gallenmüller, F., Speck, T., and Poppinga, S. (2016). Functional morphology of suction discs and attachment performance of the Mediterranean medicinal leech (*Hirudo verbana* Carena). J R Soc Interface *13*, 20160096.

31. Autumn, K. (2006). Properties, principles, and parameters of the gecko adhesive system. In Biological adhesives, A. Smith and J. Callow, eds. (Springer, Berlin), pp. 225–256.

32. Autumn, K., Hsieh, S., Dudek, D., Chen, J., Chitaphan, C., and Full, R. (2006). Dynamics of geckos running vertically. J Exp Biol *209*, 260–272.

33. Wolff, J. and Gorb, S. (2012). Comparative morphology of pretarsal scopulae in eleven spider families. Arthropod Struct Dev *41*, 419–33.

34. Weihmann, T. (2013). Crawling at high speeds: steady level locomotion in the spider *Cupiennius salei* – global kinematics and implications for centre of mass dynamics. PloS One *8*, e65788.

35. Federle, W., Barnes, W.J.P., Baumgartner, W., Drechsler, P., and Smith, J.M. (2006). Wet but not slippery: boundary friction in tree frog adhesive toe pads. J R Soc Interface *3*, 689–697.

36. Hill, I.D., Dong, B., Barnes, W.J.P., Ji, A., and Endlein, T. (2018). The biomechanics of tree frogs climbing curved surfaces: a gripping problem. J Exp Biol *221*, jeb168179.

37. Niederegger, S., Gorb, S., and Jiao, Y. (2002). Contact behaviour of tenent setae in attachment pads of the blowfly *Calliphora vicina* (Diptera, Calliphoridae). J Comp Physiol A *187*, 961–970.

38. Niederegger, S. and Gorb, S. (2003). Tarsal movements in flies during leg attachment and detachment on a smooth substrate. J Insect Physiol A *49*, 611–620.

39. Scharmann, M. (2011). Biomechanical and ecological adaptations of the pitcher plant ant *Camponotus schmitzi*. Master's thesis, Julius-Maximilians-Universität Würzburg.

40. Bohn, H.F., Thornham, D.G., and Federle, W. (2012). Ants swimming in pitcher plants: kinematics of aquatic and terrestrial locomotion in *Camponotus schmitzi*. J Comp Physiol A *198*, 465–476.